The Formation and Morphology of Highly Doped N-type Porous Silicon: Effect of Short Etching Time at High Current Density and Evidence of Simultaneous Chemical and Electrochemical Dissolutions

Suriani Yaakob[1], Mohamad Abu Bakar[1], Jamil Ismail[1],
Noor Hana Hanif Abu Bakar[1*] and Kamarulazizi Ibrahim[2]

[1]School of Chemical Sciences, Universiti Sains Malaysia,
11800 USM Pulau Pinang, Malaysia
[2]School of Physics, Universiti Sains Malaysia,
11800 USM Pulau Pinang, Malaysia

[*]Corresponding author: hana_hanif@usm.my

Abstract: *Porous silicon (PS) was successfully prepared from highly doped n-type silicon (Si) substrate. The PS was electrochemically formed within a short etching time (< 5 min) at 300 mA cm^{-2} in 1:1 (v/v) hydrofluoric acid (HF) (49%) and ethanol (95%) electrolyte. The PS surface featured both spherical and irregular shaped pores with constant average diameters regardless of etching time. However, the cross-section morphology of the PS was dependent on etching time where the structure changed from vertically arrayed columns with side branching to unbranched and smooth walls with a corresponding increase in porosity from 25 to 70%. The PS showed a trend of increasing surface roughness as the etching time was prolonged up to 180 s. However, for longer etching times, the roughness demonstrated a decrease. The conductivity of the PS was reduced as the porosity increased. These results therefore suggested the occurrence of simultaneous chemical and electrochemical dissolutions.*

Keywords: n-type Silicon, highly doped, etching time, porous silicon, morphology

1.   INTRODUCTION

Several reports have shown that a great number of parameters are involved in the formation of porous silicon (PS) prepared via electrochemical etching.[1–7] These parameters include the current density, the HF concentration, the temperature, the etching time, the type of Si and the dopant concentration. As compared to other parameters, the effect of the etching time alone on the PS formation has rarely been reported on and those that exist have focused only on low-to-medium doped n-type Si (i.e., 10^{13}–10^{17} cm^{-3}) and low current densities (i.e., 5 to 35 mA cm^{-3}).

Related studies on highly doped n-type Si (i.e., $\geq 10^{18}$ cm^{-3}) are very scarce. As an example, Aravamudhan et al.[8] prepared PS within etching times of 100–160 min and reported that pores with an average diameter of 290 nm grew

into columns with rough side walls. Meanwhile, Jeyakumaran et al.[4] reported on a trend of an increasing PS pore diameter from 2.1 to 3.5 μm as the etching time was prolonged from 10 to 20 min. However, longer etching times of 30 and 40 min caused some of the pore walls to break, thus exposing a small portion of the next layer. Milani et al.[9] prepared PS from a low doped n-type Si with an etching time in the range of 10 to 50 min. It was found that smaller pores were formed at 20 min, but they became wider and were accompanied by partially cracked walls at 30 min. Nevertheless, the pores became smaller again upon further increasing the etching time to 50 min. On the other hand, PS consisting of spongy networks with a variation of pore diameter (10–20 nm) was formed within the etching time of 1–12 min as reported by Lu and Cheng.[2]

The variation in the obtained results by previous researchers confirms the difficulties that exist when it comes to effectively controlling the PS formation, especially when low current densities and long etching times are employed. It is also obvious that the knowledge of the formation of PS from highly doped n-type Si utilising short etching times and high current densities is limited.

Preliminary work (not shown here), was carried out on the effect of current densities on the morphology and other properties of PS at a constant etching time of 300 s. It was found that the PS structures changed from spongy to columnar by varying the current density from 50 to 300 mA cm^{-2}. Although such a spongy structure of PS has been frequently reported, there exist a much lower number of observations of PS with a columnar structure. This provides a motivation to gain an improved understanding on the formation of this type of structure.

For this reason, it was decided that the present study should be performed using a current density of 300 mA cm^{-2}. By varying the etching time from 30 to 300 s, the aim is to investigate the change in PS morphology. Discussions on how other properties such as the PS thickness, pore diameter, pore density, porosity and surface roughness are influenced by the etching time are also presented. Finally, these properties are related to the electrical characteristics of the obtained PS. This knowledge is significant in order to control the PS structures depending on its application.

2.   EXPERIMENTAL

Single-side polished n-type Si wafers (doped with phosphorus) with a dopant concentration of 1.49–6.33 × 10^{18} cm^{-3}, 625–700 μm thick and <100> oriented were obtained from Siltronix Semiconductor Quality Silicon, Germany. A platinum (Pt) (99.95%) wire with a 0.013-inch diameter was provided by

Sigma-Aldrich, USA. Hydrofluoric acid (HF) (49%) was purchased from J. T. Baker, USA, and ethanol (95%) came from Chemar® Systerm, Malaysia.

First, an ohmic contact in the form of an aluminum (Al) layer on the n-type Si wafer was established. This was done by thermally depositing a layer of Al onto the unpolished side of the Si wafer by using a thermal evaporator (brand: Edwards Model Auto 306) at 5×10^{-5} Torr, and subsequently annealing at 400°C for 15 min. PS was then synthesised by electrochemical etching with the Si wafer as the anode and the Pt wire as the cathode. An electrolyte solution comprised of 1:1 (v/v) HF and ethanol was used. The etching time was varied from 30 to 300 s for the Si etching at a current density of 300 mA cm^{-2}. Sample illumination was performed on the polished side of the Si wafer using a fluorescence source connected to a D.C. switching mode power supply (brand: GW-Instek, model: SPS-606).

The morphology of the PS was characterised using a field emission scanning electron microscope (FESEM) LEO SUPRA 50 VP at an accelerating voltage of 5 kV. Average pore diameters were determined using an image analysis computer software, "analySis Docu" Version 3.2 Soft Imaging System (SIS, GmbH, Munster, Germany). The pore density of the PS surface was calculated from the number of pores per unit area (m^2), and the corresponding porosity was estimated by a gravimetric method described elsewhere.[10] The surface topography of the PS was monitored with an ULTRAObjective atomic force microscope (AFM). Image processing and surface roughness analyses were performed by exploiting the Surface Imaging System software (SIS, GmbH, Munster, Germany). Meanwhile, the electrical properties of the PS layer were studied using a Keithley Model 82 (Keithley Instruments, USA).

3.   RESULTS AND DISCUSSION

3.1   Morphology of the PS Layer

Based on the SEM micrographs, the cross-section of the PS layer can be divided into three distinct regions: the entry, middle and bottom regions. The entry region corresponds to the area in which the initial pores were formed within the surface of the Si substrate. The middle region is the area where the dissolution advanced into the bulk Si whereas the bottom region corresponds to the tip of the advancing pore bordering the bulk Si.

Figure 1 displays micrographs of the morphology of the PS layer at the entry, middle and bottom regions formed at etching times of 30, 60, 90, 180 and 300 s. At 30 s, the main pores grew in the <100> direction, which was

perpendicular to the Si surface, with side branches in the <111> direction, as depicted in Figure 1(a). This result is in agreement with that observed by Lehmann et al.[11] who prepared PS from highly doped n-type Si using an identical current density but a much shorter etching time of 6 s. This pore growth feature persisted upon increasing the etching time to 60 s, as shown in Figure 1(b).

As the etching time was further increased to 90 s, the branching structure at the wall of the bottom region of the pore disappeared, as shown in Figure 1(c). In this region, the walls were smoothed and the pores were enlarged—a behaviour that became more obvious at etching times of 180 and 300 s, as depicted in Figure 1(d–e).

Variations in the morphology of the three PS regions were mainly due to the effect of the Si dissolution process, which occurred at the Si-electrolyte interface. This dissolution process was most active at the interface. There exist two types of dissolution: viz. electrochemical and chemical. Typically, the electrochemical dissolution arises from two types of electrochemical reactions. The first is a direct electrochemical dissolution where the hydrogen-terminated Si surface is attacked by HF, thus forming unstable SiF_4 molecules. However, these unstable molecules react further with HF resulting in the more stable H_2SiF_6. The second type of dissolution is electrochemical oxidation of Si by hydroxyl ions, which leads to the formation of oxide layers. The latter is inert towards further electrochemical processes. Nevertheless, they may undergo chemical dissolution in HF solution.

It should be noted that these reactions, i.e., the electrochemical direct dissolution and oxidation, are mainly controlled by the number of holes available in the Si substrate. The electrochemical oxidation requires more holes as compared to the direct electrochemical dissolution. In this work, the progress of both reactions are dependent on the employed etching time period since the number of holes (per unit time) was fixed due to the constant current density and illumination.

The formation of pores in the <100> direction was attributed to the electrochemical dissolution, which occurred due to the holes in the Si substrate aligning themselves in response to the direction of the current line induced by a high applied current density.[12,13] The high current density induced a strong electric field that in turn exerted a polarising effect onto the Si substrate. The holes tended to accumulate at defective sites on the surface as a result of electron excitation when either the Si or dopant atom moved into the lattice or non-lattice sites of the Si crystallites. This condition encouraged the F⁻ ions in the electrolyte to the Si surface and subsequent reactions led to dissolution. These holes were preferentially accumulated at the tip of the pore bordering the bulk Si due to the

low potential energy barrier as compared to the wall area.[14,15] As a result, a greater Si dissolution was favoured at this latter site, thus forming pores with columnar structures in the <100> direction.

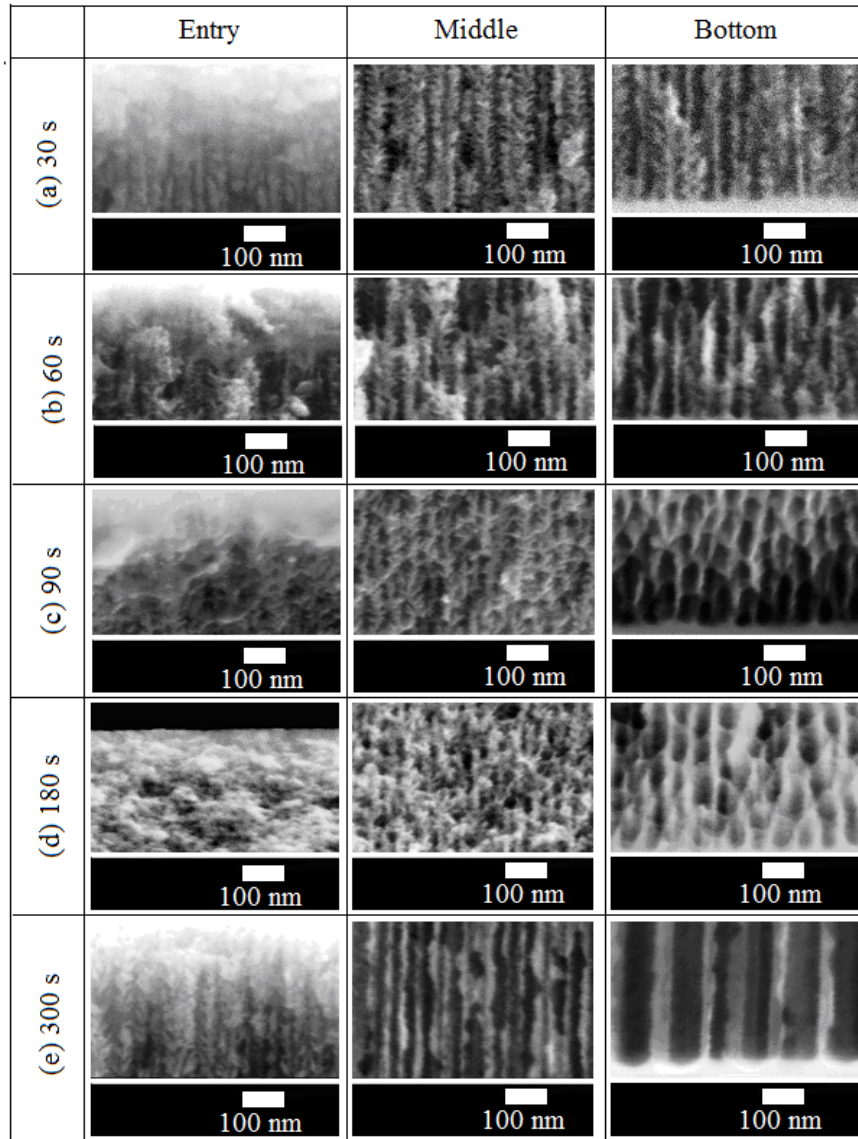|	Entry	Middle	Bottom
(a) 30 s			
(b) 60 s			
(c) 90 s			
(d) 180 s			
(e) 300 s			

Figure 1: SEM images of cross-sections for the PS substrate prepared at different etching time of (a) 30, (b) 60, (c) 90, (d) 180 and (e) 300 s.

As the electrochemical dissolution process continued, dissolution also proceeded in the <111> direction, creating side branches from the main pore. This was due to the availability of more holes in that direction. However, dissolution in this direction came to a halt once the holes depleted. This was due to the high energy barrier created by the inter-pore distance which became smaller with the progress of dissolution.

On the other hand, the enlargement of the pore diameter from the entry to the bottom region as the etching time increased was attributed to a reduction of the HF concentration with pore depth. This was caused by the limited diffusion of HF in the narrow bottlenecks close to the entry[11] as explained by Fick's Law.[16] Accordingly, the mass transport in the pore occurred only by diffusion. It is well known that diffusion is a time-dependent process, and consequently, increasing the etching time would reduce the flux of HF molecules at the bottom region. Hence, the bottom region of the pores would be filled by a lower concentration of HF electrolyte as compared to the bulk electrolyte.

Moreover, due to the low concentration of HF, the critical current density (J_{PS}) at the pore tip was reduced. This promoted oxidation on the Si surface due to the accumulation of excess holes from the constant current density and illumination employed. At this stage, dissolution could only take place chemically, and the chemical dissolution of the oxide layer occurred isotropically. As a result, the pore wall at the bottom region was smoothened and became wider. This explained the variation in the morphology of the PS formed from 30 s to 300 s as shown in Figure 1.

However, increasing the etching time to 330 s evidently separated the PS from the bulk Si. The *in-situ* separation of the PS layer occurred due to the long etching time employed, which enabled a sufficient time for the transition from pore formation to the separation of the PS layer. Solanki et al.[17] studied the formation of PS from p-type Si and also noted the occurrence of electro-polishing upon prolonged etching times with a constant current density of 150 mA cm^{-2}. Therefore, characterisations of the PS prepared beyond 300 s were abandoned.

The effect of the etching time on the thickness and etching rate of the PS layer is shown in Figure 2. A linear correlation displaying the thickness enhancement from 10 to 52 µm with an increasing etching time can be observed. Such a trend was in agreement with the results by Arita and Sunohara[18] who attained a (1–12 µm) porous layer from an electrochemical etching of highly doped n-type and p-type Si within a smaller etching time span (i.e., < 70 s). Their results were found for low-to-medium (16–100 mA cm^{-2}) current densities. In addition, Kumar and Huber[19] also reported on a similar trend obtained from p-

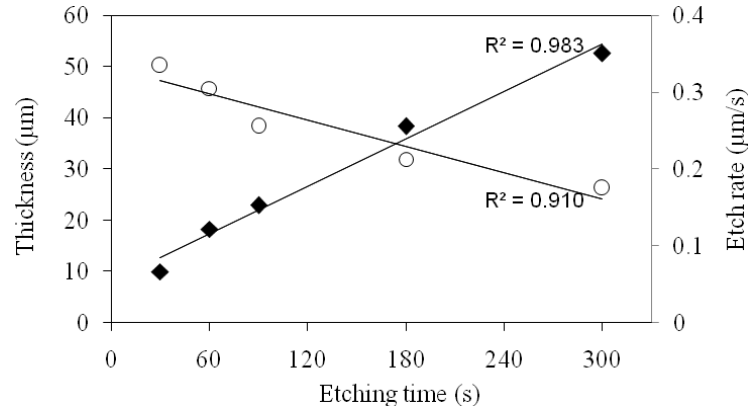type Si with longer etching times, ranging from 50–550 min and a lower but constant current density of 12.5 mA cm^{-2}.

Figure 2: Thickness (◆) and etch rate (○) of the PS etched at 300 mA cm^{-2}, as a function of etching time.

In contrast to the thickness, the etching rate showed an opposite trend. This suggests that short etching times led to significant pore growth and the underlying reason was thought to be a direct attack of F$^-$ ions on the Si atoms. However, as the etching time increased, another process of dissolution, i.e., chemical dissolution, began to dominate.[20] This process was common at the pore wall and suppressed the reaction at the tip of the pore. Hence, the etching rate at the pore tip became reduced and only pore propagation occurred slowly. Consequently, the inter-pore distance becomes narrower with an increasing etching time.

Figure 3 shows SEM surface images of PS formed at etching times of (a) 30, (b) 90, (c) 180 and (d) 300 s. The dark spots on the images are attributed to the pores formed, whereas the white area corresponds to the remaining Si. The pores are spherical and irregular in shape, and are randomly distributed on the PS surface. Results also demonstrate that there is no apparent effect of the etching time on the pore shape. This is in agreement with the work of Milani et al.,[9] who prepared PS from a low doped n-type Si with an etching time that ranged from 10 to 50 min at 25 mA cm^{-2}.
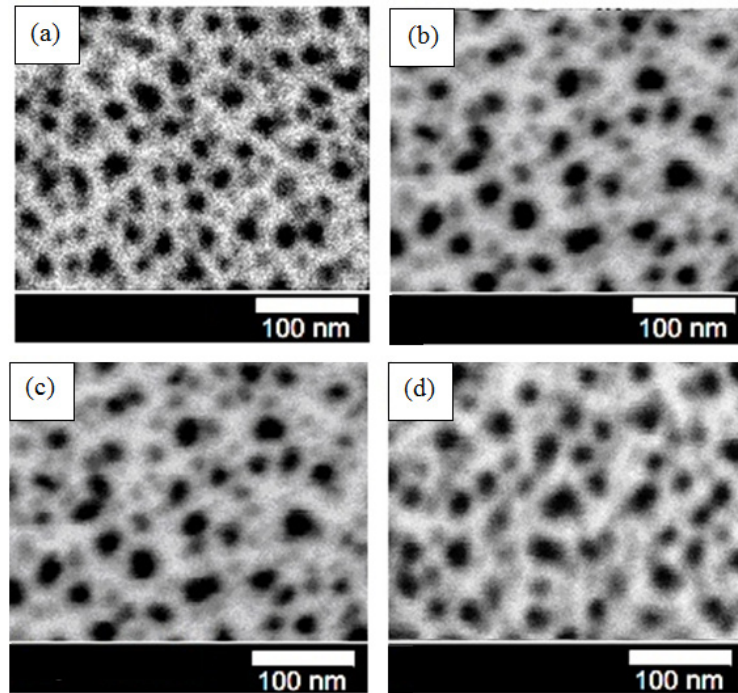
Figure 3: SEM surface images of PS formed at etching times of (a) 30, (b) 90, (c) 180 and (d) 300 s.

Figure 4 depicts the correlation of the average pore diameter as well as the pore density of the PS as a function of the etching time. There is no significant change in the pore diameter as the etching time was increased, and the average pore diameter is 19.00 ± 2.62 nm for all employed etching times. The results suggest that the dissolution of Si took place uniformly in the bulk Si. As the etching time was increased, the dissolution process continued perpendicularly towards the bulk Si. This was also reflected by the constant pore density, as plotted in Figure 4. The uniformity obtained was attributed to the almost equal number of holes that were generated, resulting from the constant applied current density and illumination.

Several observations have been reported by Jeyakumaran et al.[4], who carried out electrochemical etching on a low doped n-type Si at longer etching times, i.e., of 10 to 40 min, with a current density of 30 mA cm^{-2}. In their case, the pore diameter reached a maximum at 20 min. However, it then decreased as the etching time was prolonged up to 40 min. The increment in pore diameter of the former case was the result of active dissolution of Si at the pore wall which enlarged the pore size, and consequently reduced the inter-pore distance. This may be due to the fast dissolution on the Si surface via a direct attack of HF

followed by oxidation. Such a rapid dissolution further caused the pore wall to break as longer etching times were employed. This exposed a small portion of the underlying PS layer with smaller pore diameters. Thus, a reduction in pore size was observed. Further studies are required to better understand the difference between the observations of Jeyakumaran et al. as compared to those from the present study.
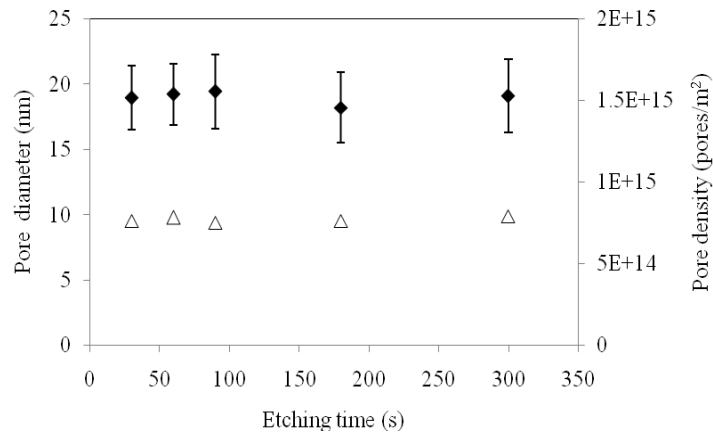

Figure 4: Pore diameter (◆) and pore density (△) as a function of etching time.

In a subsequent step, further analyses were conducted on the surface inter-pore distance of the etched Si. Figure 5 depicts a plot of the average inter-pore distance as a function of the etching time. No apparent effect of the etching time could be seen on the inter-pore distance; the trend thus resembled those of the pore diameter and pore density as previously shown in Figure 4. The average distance between the neighboring pores is 14.68 ± 2.94 nm and as a result, it was obvious that the dissolution of Si was consistently perpendicular to the bulk Si for all studied etching times. Once the pores were formed, the remaining surface Si became inert from further direct dissolution, leading to the observed constant pore density and pore diameter. As the etching time was increased, the dissolution proceeded into the bulk Si, affecting further propagation of the pores.
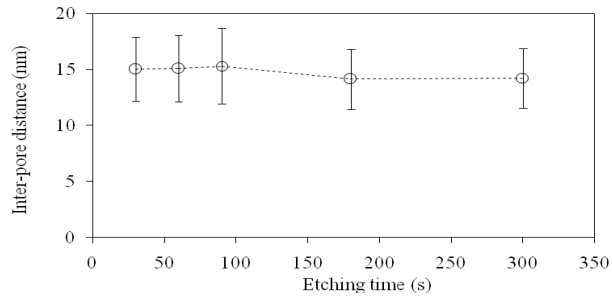
Figure 5: Inter-pore distance of PS as a function of time.

3.2   Porosity

Porosity is defined as the amount of voids within the PS layer and was observed to increase from 25% to 70% with an augmentation of the etching time, as shown in Figure 6. The increment in the porosity was caused by the enhancement of the Si dissolution. The mass of dissolved Si increased due to either active electrochemical or chemical dissolution with the etching time. This is believed to occur at the PS-Si interface, which is consistent with the previous observations concerning the pore diameter, pore density and the inter-pore distance, as discussed earlier. Moreover, such a trend is in agreement with those reported by Kumar and Huber.[19]
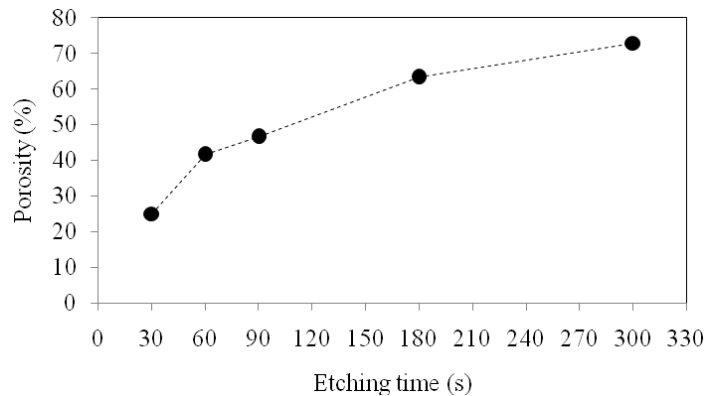

Figure 6: Porosity as a function of etching time.

3.3   Surface Roughness of the PS Surface

Figure 7 shows the representative atomic force microscopy (AFM) images corresponding to (a) bulk Si and PS prepared at etching times of (b) 30, (c) 60, (d) 90, (e) 180 and (f) 300 s. Bulk Si exhibited a smooth surface

morphology, as revealed by AFM micrographs shown in Figure 7(a). However, electrochemical etching during the production of PS generated several small bumps on the surface. The formation of such bumps is possibly due to the surface relief of the Si nanostructures after the etching process. The number of bumps on the surface of the PS gradually increased with the etching time and then abruptly decreased after 300 s of etching, as shown in Figure 7(b–f). Figure 8 presents a plot of the roughness value (rms) of the PS surface as a function of the etching time. As the etching time was prolonged, the surface roughness increased from 5.36 nm to 17.25 nm before decreasing to 5.20 nm. In comparison, the roughness of the neat Si surface was 3.10 nm.
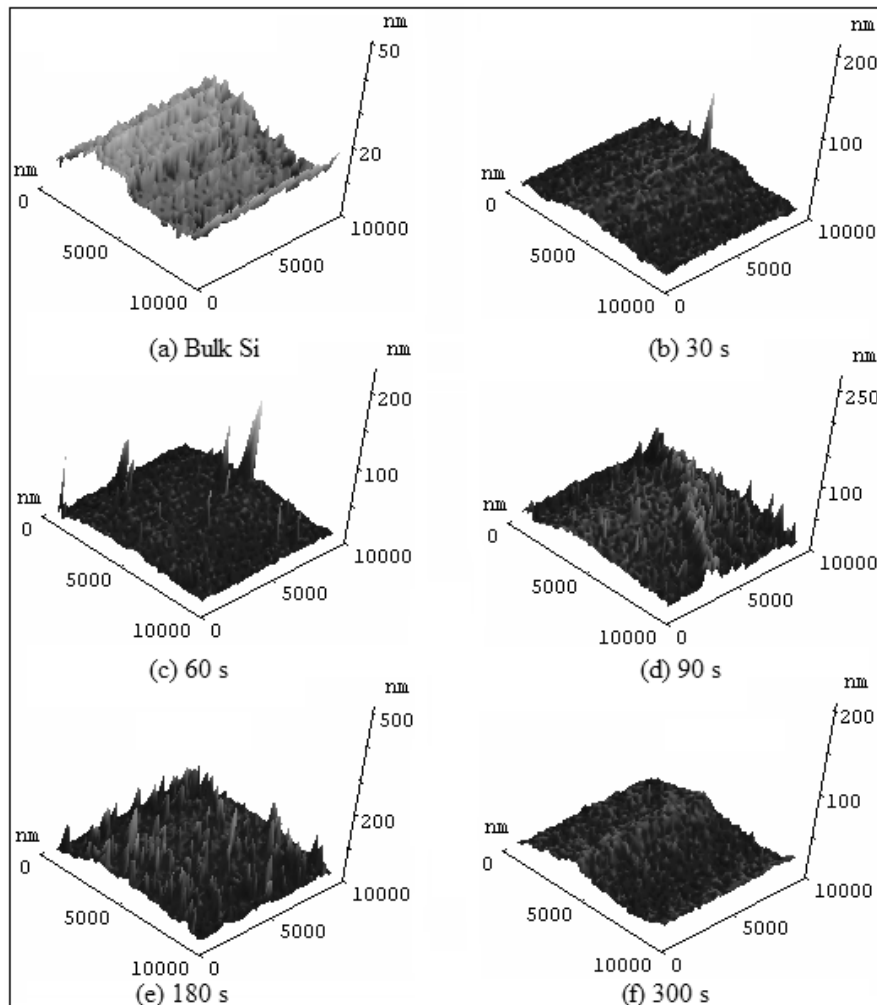

Figure 7: AFM images of (a) bulk Si and PS surface (b–f) as a function of etching time.
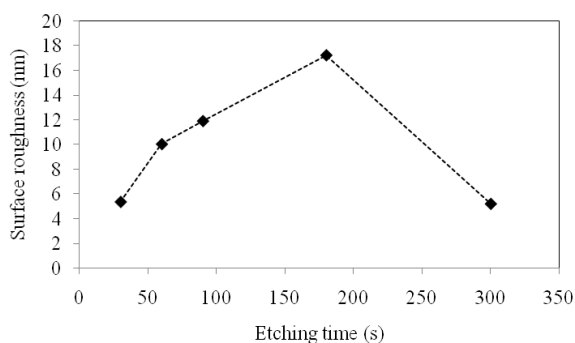
Figure 8: The surface roughness of PS as a function of etching time.

As explained earlier, the direct electrochemical dissolution is perpendicularly orientated with respect to the bulk Si. The remaining exposed Si atoms were only susceptible to electrochemical oxidation. Therefore, the smoothening of the PS surface upon prolonged etching was attributed to the chemical dissolution that occurred slowly and evenly at the peak of the bumps. Consequently, a consistent chemical dissolution may have resulted in bumps of almost uniform height. The increasing number of these uniform bumps caused the amount of their non-uniform counterparts to decrease. Hence, the PS surface became somewhat smoothened.

3.4 Electrical Properties of the PS Layer

A forward bias voltage was applied to a sandwich structure of Al/PS/n-Si/Al, and Figure 9 represents the typical forward I-V characteristics of the PS as a function of the etching time. The conductivity of the PS layer decreased gradually with increasing etching time from 30 s to 300 s. On the other hand, the bulk Si demonstrated a higher conductivity compared to the etched Si. This is in agreement with the results obtained by Milani et al.,[9] who suggested that the decline in the conductivity of PS with the etching time was due to a limited mobility of charge carriers in the increasingly porous PS layer. The present study supports this statement since trends of increasing thickness and porosity were seen for the obtained PS layer when the etching time was prolonged.
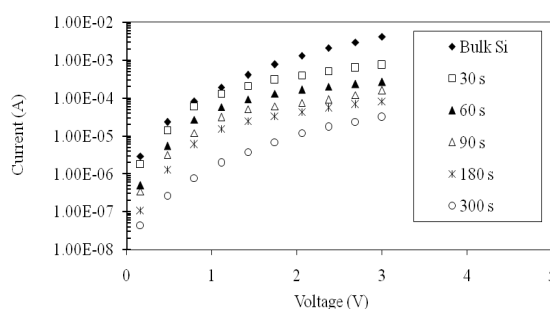
Figure 9: I-V characteristics of the Al/PS/bulk Si/Al as a function of current density.

4.   CONCLUSION

PS was successfully prepared from highly doped n-type Si substrates under periods of short etching times, from 30 to 300 s and at a high current density of 300 mA cm^{-2}. The morphology of the as-prepared PS changed from a narrow columnar structure with side branching at 30 s to larger, non-branched columns at 300 s. At 330 s, however, electro-polishing set in, signifying that the critical current density (J_{ps}) had dropped below the applied current density. The pore diameter and inter-pore distance remained practically unchanged while the porosity increased as the etching time was prolonged. The PS surface showed an increasing trend with regard to the roughness, i.e., from 5.36 to 17.25 nm, upon increasing the etching time from 30 to 180 s. However, the roughness decreased to 5.20 nm when the etching time was further increased to 300 s. The above results suggest that the electrochemical and chemical dissolutions occurred concurrently, albeit at different rates.

The consistent direct electrochemical dissolution propagated pores into the bulk Si with occasional branching as the etching time was increased. The then exposed Si atoms were subjected to electrochemical oxidation which led to an oxidised surface, ultimately giving rise to a PS with columnar structures with similar pore diameters, shapes and inter-pore distances etc. However, the chemical dissolution caused a smoothening of the pore wall with a subsequent enlarging of the pore bottom as well as of the PS surface. Meanwhile, the conductivity of the PS layer was reduced with increasing etching times due to the limited mobility of charge carriers as the porosity of the PS layer increased.

5. ACKNOWLEDGEMENTS

6. REFERENCES

1. Balagurov, L. A. et al. (2006). Formation of porous silicon at elevated temperatures. *Electrochim. Acta*, 51, 2938–2941.

2. Lu, J. & Cheng, X. (2008). Effect of etching time on porous silicon formation. *ECS Trans.*, 11(11), 9–17.

3. Long, Y., Ge, J., Ding X. & Hou, X. (2009). Temperature: A critical parameter affecting the optical properties of porous silicon. *J. Semicond.*, 30(6), 063002, DOI:10.1088/1674-4926/30/6/063002.

4. Jeyakumaran, N., Natarajan, B., Ramamurthy, S. & Vasu, V. (2007) Structural and optical properties of n- type porous silicon-effect of etching time. *Inter. J. Nanosci. Nanotech.*, 3(1), 45–51.

5. Mehra, R. M., Agarwal, V., Jain, V. K. & Mathur, P. C. (1998) Influence of anodisation time, current density and electrolyte concentration on the photoconductivity spectra of porous silicon, *Thin Solid Films*, 315, 281–285.

6. Lehmann, V. (2002) *Electrochemistry of silicon: Instrumentation, sciences, materials and applications*. Weinhein, Germany: Wiley-VCH Verlag.

7. Zhang, X. G. (2001) *Electrochemistry of silicon and its oxide*. New York: Kluwer Academic/Plenum Publishers.

8. Aravamudhan, S. et al. (2007). Porous silicon templates for electrodeposition of nanostructures. *App. Phys. A*, 87, 773–780.

9. Milani, S. D. et al. (2006). The correlation of morphology and surface resistance in porous silicon. *J. Opto. Adv. Mater.*, 8(3), 1216–1220.

10. Plessis, M. (2007). Properties of porous silicon nano-explosive devices. *Sens. Actuators A*, 135, 666–674.

11. Lehmann, V., Stengl, R. & Luigart, A. (2000). On the morphology and the electrochemical formation mechanism of mesoporous silicon. *Mater. Sci. Eng. B*, 69(70), 11–22.

12. Chuang, S. F., Collins, S. D. & Smith, R. L. (1989). Preferential propagation of pores during the formation of porous silicon: A transmission electron microscopy study. *App. Phys. Lett.*, 55(7), 675–677.

13.   Chuang, S. F., Collins, S. D. & Smith, R. L. (1989). Porous silicon microstructure as studied by transmission electron microscopy. *App. Phys. Lett.*, 55(15), 1540–1542.
14.   Smith, R. L. & Collins, S. D. (1992). Porous silicon formation mechanisms. *J. App. Phys.*, 71(8), RI–R22.
15.   Kumar, P., Hofmann, T., Knorr, K. & Huber, P. (2008). Tuning the pore wall morphology of mesoporous silicon from branchy to smooth, tubular by chemical treatment. *J. App. Phys.*, 103(2), 024303-1-024303-6, DOI: 10.1063/1.2829813.
16.   Thonissen, M. et al. (1996). Depth inhomogeneity of porous silicon layers. *J. App. Phys.*, 60(5), 2990–2993.
17.   Solanki, C. S., Bilyalov, R. R., Bender, H. & Poortmans, J. (2000). New approach for the formation and separation of a thin porous silicon layer. *Phys. Status Solidi A*, 182, 97–102.
18.   Arita Y. & Sunohara, Y. (1977). Formation and properties of porous silicon film. *J. Electrochem. Soc.*, 124(2), 285–295.
19.   Kumar P. & Huber, P. (2007). Effect of etching parameter on pore size and porosity of electrochemically formed nanoporous silicon. *J. Nanomater.*, article ID 89718, DOI: 10.1155/2007/89718.
20.   Carstensen, J., Christophersen, M. & Foll, H. (2000). Pore formation mechanisms for the Si-HF system. *Mater. Sci. Eng. B*, 69(70), 23–28.